RSC Advances

PAPER

View Article Online
View Journal | View Issue

Cite this: *RSC Adv.*, 2024, **14**, 6805

How surface-to-volume ratio affects degradation of magnesium: *in vitro* and *in vivo* studies

Jiang Sun,†*[abc] Shan-Shan Liu,†*[abc] Da Zou,†*[abc] Xuan He,*[abc] Zhang-Zhi Shi*[d] and Wei-Shi Li *[abc]

Despite the many studies carried out over the past decade to determine the biodegradation performance of magnesium and its alloys, few studies focused on the effect of altered surface area to volume ratio on *in vitro* and *in vivo* degradation rate and osteogenesis. Here, high purity magnesium cylindrical rods with gradient of surface area to volume ratio were processed by excavating different numbers of grooves on the side surface. The immersion test in SBF solution and the rat femoral condylar bone defect model were used to evaluate the degradation of magnesium rods *in vitro* and *in vivo*, respectively. We demonstrated that, the increased number of grooves on the HP magnesium surface represented a decrease in the percentage of residual volume over time, not necessarily an increase in absolute degradation volume or a regular change in corrosion rate. Furthermore, there were strong linear correlations between the relative degradation volume and the initial surface-to-volume ratio of HP magnesium rods both *in vitro* and *in vivo*. The difference in the slope of this relationship *in vitro* and *in vivo* might help to determine the possible range of *in vivo* degradation rates *via in vitro* data. In addition, the corrosion rate is more suitable for evaluating bone formation surrounding the different HP magnesium rods. Our findings in this work may facilitate adjusting the *in vivo* degradation and osteogenesis of different kinds of orthopedic implants made of the same magnesium-based material, and thus, accelerate the clinical popularization and application.

Received 29th December 2023
Accepted 12th February 2024

DOI: 10.1039/d3ra08927d

rsc.li/rsc-advances

1 Introduction

With the continuous growth in worldwide orthopedic surgery volume[1] and higher requirements for healing quality, a series of biomaterials, including biopolymers, bioceramics, and biometals, have been developed for bone repair application in recent decades.[2] Among them, magnesium and its alloys have received more attention owing to their natural degradability, thereby requiring no need for secondary surgical removal. *In vitro* experiments indicated that Mg^{2+} can facilitate bone repair through various pathways, *e.g.*, promoting the osteogenic differentiation of periosteum-derived stem cells (PDSCs) *via* activating the CGRP receptor (consisting of CALCRL and RAMP1)[3] as well as the proliferation and osteogenic differentiation of MSC by sequentially activating MAPK/ERK and Wnt/β-catenin signaling pathways.[4] Furthermore, based on the promising outcomes in animal models and clinical follow-up,[5–10] MgYReZr screws first obtained a Conformité Européene (CE) mark in Germany in 2013,[11] and soon afterwards, magnesium-based screws for vascularized bone flaps and radius fractures fixation were approved by the China FDA (CFDA) and the Korea Food and Drug Administration (KFDA) respectively.[12,13] However, since its first application in traumatic surgery in 1900,[14] concerns have persisted regarding the rapid degradation of magnesium in the human body. Thus, alloying or optimized manufacturing methods and post-processing techniques such as heat treatment have been employed to magnesium-based materials to control the degradation behavior through adjusting the purification, composition and microstructure, including the grain size and texture of the base material.[15] In addition, surface coating technology has been developed to protect the magnesium matrix from direct contact with body fluid. It was widely believed that the degradation of magnesium and its alloys must be tailored following a suitable manner before osteosynthesis application, which should satisfy (i) an adequate stability during fracture healing and (ii) a moderate and homogeneous degradation performance in equilibrium with the bone healing process.[2] Fast or uncontrolled degradation is associated with strong hydrogen and ion release and severe pH changes, which can lead to undesirable

[a]*Peking University Third Hospital, Beijing, 100191, China. E-mail: sjdoctor@pku.edu.cn; zd_puth@163.com; hexuanpeter@163.com; puh3liweishi@163.com; 1039165305@qq.com*

[b]*Engineering Research Center of Bone and Joint Precision Medicine Department of Orthopedics, Beijing, 100191, China*

[c]*Beijing Key Laboratory of Spinal Disease Research, Beijing, 100191, China*

[d]*University of Science and Technology Beijing, Beijing, 100083, China. E-mail: ryansterne@163.com*

† Jiang Sun, Shan-Shan Liu and Da Zou contribute equally to this manuscript and are considered as co-first authors.

clinical outcomes, conversely, slow degradation can hinder the ingrowth of the new bone.[16] Therefore, for magnesium-based materials under development, it is particularly important for researchers to accurately predict their degradation rate in the human body and adjust process parameters of surface treatment or alloying and so on accordingly.

The degradation behavior of magnesium-based materials can be evaluated through both *in vivo* and *in vitro* methods. Considering the long testing times, high cost, surgical procedures and ethical issues of *in vivo* model when using as preliminary screening and evaluation of the degradation behavior, establishing a simple and highly reproducible connection between *in vitro* and *in vivo* test results is hence important for further clinical applications of Mg and its alloys. The various techniques available to measure corrosion *in vitro* are grouped into two categories: (i) unpolarized and (ii) polarized. The former are all inexpensive and easily performed including static or dynamic immersion tests with H_2 evolution measurement, pH monitoring and weight loss measurement of specimens, while the latter are simple to perform and highly reproducible including potentiodynamic polarization, electrochemical impedance spectroscopy. The difference between these methods relates to the presence of a driving force (*i.e.* electrochemical polarization) which is applied or measured during the test.[17] In order to facilitate comparison, analysis and standardization of experimental results obtained by different researchers, ASTM has already published standard for *in vitro* corrosion evaluation of absorbable metals, which provided guidelines for general test conditions and monitoring requirements (F3268). However, due to differences in the selection of immersion solution, testing duration, and testing methods in practical operation, a large range of results can be achieved even for the same alloy. Hence, researchers will find it difficult to directly refer to the *in vivo* performance of magnesium-based alloy with similar *in vitro* degradation rates reported in literature to predict their own newly developed materials. Actually, even if the immersion solution used *in vitro* tests is limited, Martinez *et al.*[15] reported that the *in vitro* and *in vivo* differences in degradation rates between different magnesium alloys are significant (conversion factor: 1.1 of pure Mg, 8.9 of Mg–1.34Ca–3Zn). In theory, due to differences in chemical composition, grain size, texture, type, size and distribution of the second phase, and dislocation density among different alloys, the impact of differences in the internal and external environments on their degradation behavior also varies.[18] As a result, it is almost impossible to summarize the conversion factor or mathematical formula of *in vitro* and *in vivo* degradation rates applicable to all magnesium-based materials.

Once the biological safety and osteogenic induction of a specific magnesium-based material are verified, it is often hoped to be used in more implant devices in the future. Yet, the requirements for the retention time of magnesium-based fixations and repair scaffolds may vary depending on the surgical procedure, implantation site, and functions in clinical practice. Therefore, if the possible degradation rate of the same material used in other implant devices can be inferred from existing *in vitro* and *in vivo* degradation data, it can significantly reduce the development time and cost of magnesium-based implants, and make it easier to meet differing clinical needs.

Surgeons often focus on residual volume ratio of magnesium-based alloy after implantation at specific time points due to concerns about the reliability of early fixation. For the same magnesium-based material for different applications, previous literature-based analyses have suggested that the implant location has little impact on its degradation rate in the field of orthopedics,[15] thus the surface area to volume ratio are rightly considered a determinant of the residual volume at specific time points. However, considering the dynamic changes in volume and surface area during the degradation process *in vivo*, as well as the active regulation and transportation of tissues around the implants, when applied to different devices, residual volume cannot be accurately predicted solely by considering the differences in surface area and volume parameters before implantation based on previous degradation data of the same material.[15] How and to what degree the surface-area-to volume ratio differences in various implants can affect the degradation behavior *in vivo* remains incompletely clear so far.

Recent evidence suggested that the therapeutic effect of Mg^{2+} shows a significant concentration- and stage-dependent behavior.[19] For example, Mg^{2+} in the culture medium with concentration higher than 0.5×10^{-3}M could act as a Ca^{2+} antagonist and inhibit the production of collagen and other raw materials so that impaired the bone biomineralization degree.[20] In another report, Qiao *et al.*[21] found that continued exposure of Mg^{2+} lead to the excessive osteoclastogenesis and bone destruction due to the overactivation of NF-κB signaling in macrophages. However, due to limitations such as difficulty in real-time tracking of degradation rate *in vivo*,[22] it is difficult to quantify the relationship between the *in vivo* degradation performance and the osteogenic effect of Mg. Based on this, this experiment further aims to examine whether the difference in degradation rate of HP magnesium with gradient of surface area-to-volume ratio is sufficient to cause changes in the osteogenic effect of HP magnesium rods, then quantify the differences.

This current study directly compares the performance of four different designs of HP magnesium bone defect implants *in vitro* and in rat femoral condylar defects, with the intention of identifying the effect of surface area-to-volume ratio on the degradation behavior and *in vivo* biological effects. The use of different number of grooves to set the group is to simulate the effect of different number of threads of bone screws in clinical application. Ultimately, the aim of this work is to facilitate the clinical promotion of well-established magnesium-based materials and the screening and improvement of newly developed materials and processing techniques for future investigators.

2 Materials and methods

2.1. Materials

The high purity magnesium (HP Mg, 99.99 wt%) cylindrical rods were supplied by Beijing Shiyue Advanced Material

Technology Co. Ltd, China. The cylindrical rod had a diameter and height of 3 mm and 3.5 mm, which was designed according to the bone defect repair model for rat lateral femoral condyle.[23] Gradient of surface area-to-volume ratio was achieved by excavating different numbers of grooves with a depth of 0.5 mm and a width of 0.5 mm on the side surface of the magnesium cylindrical rods. The HP magnesium cylindrical rods with 0, 1, 2, and 4 grooves (hereafter 0 g, 1 g, 2 g, 4 g) correspond to the surface area of 47.13 mm^2, 53.41 mm^2, 59.69 mm^2, 72.25 mm^2, the volume of 24.74 mm^3, 22.38 mm^3, 20.02 mm^3, 15.31 mm^3 and the surface area-to-volume ratio of 1.91, 2.39, 2.98, 4.32, respectively. Design of four types of cylindrical rods were illustrated in Fig. 1. According to the pre-design of the sample, the small cylinder with different shapes is drawn by Auto CAD drawing software and imported into the five-axis milling machine automatically controlled by the computer for precision machining. In order to protect the sample surface from oxidation, the whole processing process is carried out in an argon atmosphere. Samples were ultrasonically cleaned and sterilized using 29 kGy of ^{60}Co radiation before implantation.

2.2. Immersion tests

In vitro degradation was studied by immersion of samples in SBF (simulated body fluid) solution for 12 and 24 weeks at 37 °C, pH 7.4, and the SBF was replaced every 2 days. The specific ion component concentration is as follows: 142.0 mM Na^+, 5.0 mM K^+, 1.5 mM Mg^{2+}, 2.5 mM Ca^{2+}, 148.8 mM Cl^-, 4.2 mM HCO_3^-, 1.0 mM HPO_4^{2-}, 0.5 mM SO_4^{2-}. The ratio of solution volume to the sample area was set to 20 mL cm^{-2} according to the ASTM-G31-72 standard. At each time point, the samples were immersed in 200 mg mL^{-1} CrO_3 for 1 min at 80 °C then cleaned three times using distilled water. The *in vitro* corrosion rate (CR) is calculated according to eqn (1),

$$CR = 8.76 \times 10^4 \Delta W / A t \rho \quad (1)$$

where ΔW is the weight loss, A is the original surface area, ρ is the density of the sample and t is the time of immersion. Four parallel samples were measured for each group.

2.3. Preliminary animal study

2.3.1. Animal model and study design. All animal operations and experiments were approved by the Peking University Institutional Review Board Office (LA2019209). A total of 16 male Sprague Dawley (SD) rats aged 10–12 week old, weighing 270–300 g, were purchased from Beijing Vital River Laboratory Animal Technology Co., Ltd and maintained in the specific pathogen-free facilities. A cylindrical bone defect repair model for rat lateral femoral condyle was established. After being anaesthetized with 3% isoflurane (RWD, China), the rats were placed in the supine posture and the skin overlying the bilateral knee joints was prepared and strictly disinfected using iodophor and ethyl alcohol. A 12 to 15 mm lateral parapatellar incision was made to expose the lateral femoral condyle. With the knee positioned in 45° flexion, a bone tunnel of 3 mm in diameter and 3.5 mm in depth was created using a sterile dentistry drill. After irrigating with sterile saline solution, a cylindrical HP magnesium rod was carefully implanted into

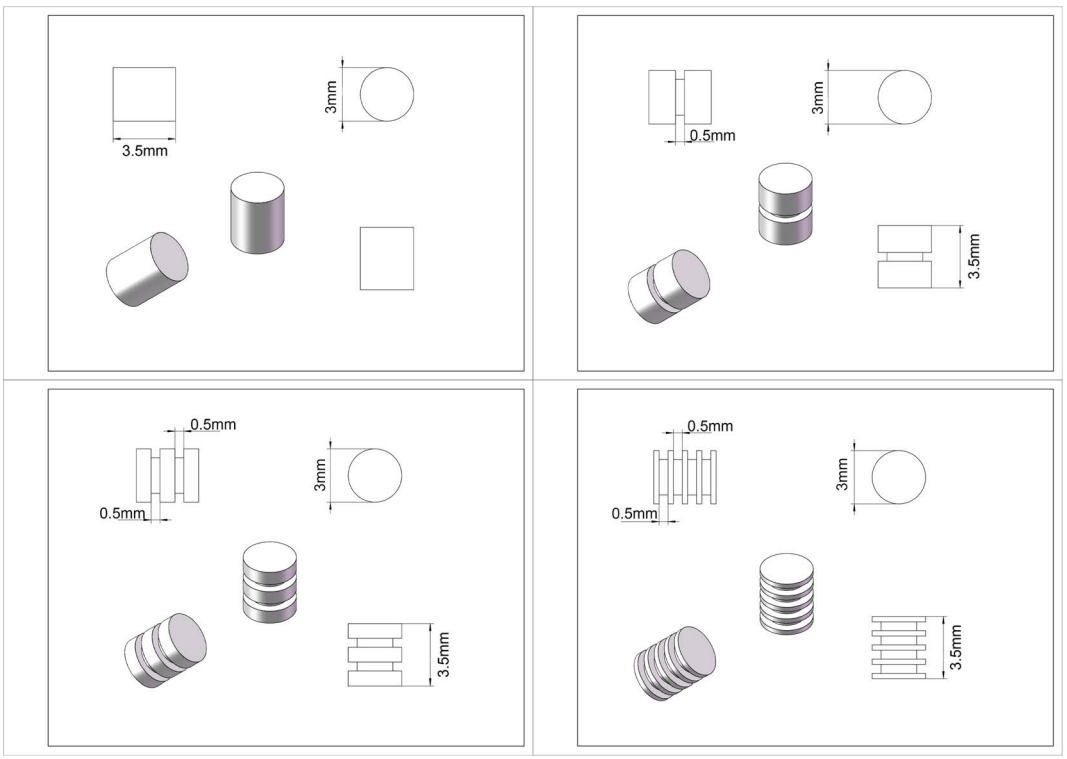

Fig. 1 Schematic design of HP magnesium rods with dimensions.

the bone defect site, then the incision was sutured layer by layer. Animals were sacrificed and their femurs were removed and dissected free of adherent soft tissue at 12 or 24 weeks after surgery. For each experimental group or time point (0 g, 1 g, 2 g, 4 g at 12 or 24 weeks) contained 4 knee joints. Signs of limping, joint swelling, subcutaneous emphysema were recorded daily before sacrifice.

2.3.2. Micro-computed tomography (Micro-CT) evaluation. The *in vivo* degradation of HP magnesium cylindrical rods and new bone formation in the defect region of femoral condyles were monitored by Micro-CT device (Siemens INVEON MM, Germany). The scanning parameters were as follows: 70 kV and 400 μA in the X-ray tube, 13 μm scan resolution, and 400 ms exposure time. Multimodal three-dimensional (3D) visualization software (Siemens INVEON MM, Germany) was used for 3D reconstruction of the images. Bone tissue and implant materials were distinguished based on HU ranges according to visual evaluation as well as previously study,[24] and the region of interest (ROI) was defined as the cylindrical area situating at the initial bone defect.

2.3.3. Histological analysis. Histological analysis was carried out to evaluate the peri-implant osseointegration at 12 and 24 weeks after surgery. After completing the Micro-CT analysis, the specimens were fixed with 4% paraformaldehyde (Yili FineChemical, China) for 48 h and decalcified in 15% ethylenediaminetetraacetic acid solution for 8 weeks. The decalcified femoral bones were dehydrated and embedded in paraffin, and then sectioned with a thickness of 5 μm. The slides were stained with hematoxylin and eosin (H&E, Solarbio, China) and Masson trichrome staining (Solarbio, China) after dewaxing and rehydrating in a graded series of ethanol according to routine protocols.

2.4. Statistical analysis

Statistical analyses were performed with SPSS software (version 24.0; IBM). All data are presented as means ± standard deviation. Data analysis and correlation were carried out using independent two-sample *t*-test (between two groups), one-way ANOVA with Tukey's *post hoc* test (multiple comparisons between two groups) and Pearson's correlation analysis, as well as linear regression analysis. Differences were determined to be statistically significant when $p < 0.05$.

3 Results and discussion

3.1. Evaluation of effects of the number of grooves on *in vitro* and *in vivo* degradation performance

Prior to discussion of the results, it should first be stated that the aim of this work is not to find a method to predict *in vivo* degradation rate through *in vitro* experiments, but to find out how the degradation of implants in bone tissue changes when the initial surface area and volume changes, and whether this trend is consistent *in vivo* and *in vitro*.

The weight changes during immersion tests as well as the volume changes calculated from Micro-CT scans at 12 and 24 weeks post-implantation were recorded to evaluate *in vitro* and *in vivo* degradation performance. In all the experimental rats, no significant restriction of movement of both lower limbs was found after 1 week of recovery except for 2 cases of subcutaneous cysts caused by infection.

It is easy to find that the increased number of grooves accelerates, for the short and long term, the relative degradation rate (absolute degradation volume divided by initial volume), not only *in vitro* but also *in vivo* (Fig. 2a and b). However, more grooves did not necessarily mean that more absolute volume of magnesium was degraded. This was true both *in vivo* and *in vitro*, but the trends were not the same. After 12 weeks' immersion *in vitro*, 4 g rods exhibited the highest volume loss of 10.2 ± 0.2 mm^3, followed by the 9.50 ± 0.3 mm^3 of 0 g rods. The other two groups did not have a statistically significant difference. However, at the same time, 2 g and 4 g rods degraded the largest volume *in vivo*, and 0 g and 1 g rods degraded relatively little volume (Fig. 2c). In the early stage of implantation, the greater number of grooves represented a lager absolute degradation volume to some extent which may be attributed to a larger initial surface area, but over time, this trend disappeared (Fig. 2d).

The surface integrity of machined components, encompassing roughness, residual stress, and microstructure, significantly impacts their corrosion resistance. Variations in surface integrity, including the presence of tensile/compressive residual stress, microhardness, twinning, and surface roughness, are closely linked to the cutting parameters.[25–27] Desai *et al.*[28] demonstrated that the feed rate emerges as the most influential factor affecting the average surface roughness value, which subsequently plays a pivotal role in determining degradation rates. Uddin *et al.*[29] reported that machined surfaces optimized under specific parameters exhibited approximately a 9% increase in corrosion potential and a notable 54% reduction in corrosion density and rate compared to their as-received counterparts. In this study, identical cutting parameters were employed for sample preparation, and only the effect of specific surface area on degradation performance was evaluated. We suspect that this phenomenon is mainly related to the difference in the dynamic change rate of surface area of magnesium rods with different designs due to uneven pitting corrosion as well as the stress corrosion *in vivo*.

Interestingly, as the most commonly used parameter to evaluate the degradation rate, the effect of different number of grooves on the corrosion rate of magnesium rods presented a completely different law. The effect of the design parameters on corrosion rate has been often disregarded in prior research studies, which implies that a single material is considered to have a fixed average corrosion depth per unit surface area at a certain implant site during the same observation period. However, differences in corrosion rates were observed in both *in vivo* and *in vitro* environments for each group of samples whether at 12 or 24 weeks as shown in Fig. 3.

In general, the corrosion rate of magnesium rods *in vitro* decreased with the increase of the number of grooves. However, only when the number of grooves was increased to four, the corrosion rate *in vivo* would be significantly decreased at 24 weeks (Fig. 3a and b). This means that when developing

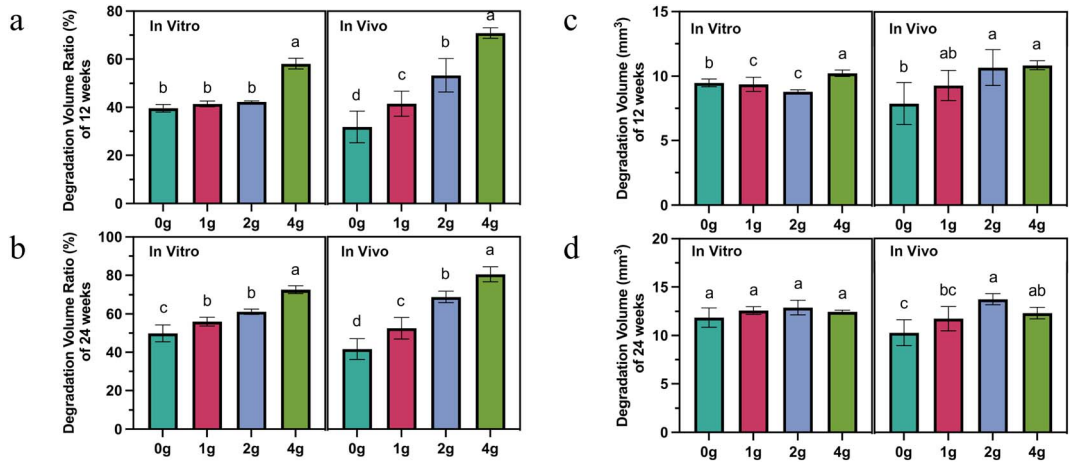

Fig. 2 The *in vitro* and *in vivo* degradation performance of the HP magnesium with different designs at 12 and 24 weeks post-operation. (a) The relative degradation volume of 12 weeks ($n = 4$). (b) The relative degradation volume of 24 weeks ($n = 4$). (c) The absolute degradation volume of 12 weeks ($n = 4$). (d) The absolute degradation volume of 24 weeks ($n = 4$). One-way ANOVA with Tukey's *post hoc* test. Columns significantly different letter ($p < 0.05$) to each other would be labeled with different letters.

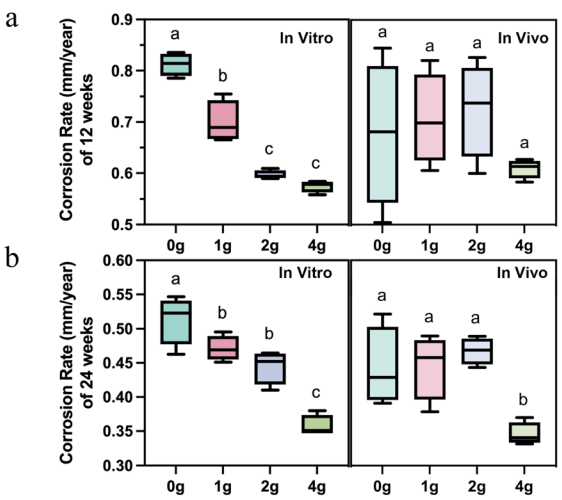

Fig. 3 The *in vitro* and *in vivo* corrosion rate of the HP magnesium rods with different designs at 12 (a) and 24 weeks (b) post-operation ($n = 4$). Columns significantly different letter ($p < 0.05$) to each other would be labeled with different letters.

orthopedic implants with different forms of the same magnesium-based material, the corrosion rate of one implant cannot be directly used, but rather requires conversion or selection of other descriptive parameters just like relative degradation rate mentioned above.

In addition, the degradation of HP magnesium rods with different designs (0 g, 1 g, 2 g, 4 g) in SBF solution and femoral condyle shared similar fast-to-slow degradation behavior (Fig. 2), which was in line with previous findings.[30]

Following are the main corrosion reactions on pure Mg:[31]

$$Mg \rightarrow Mg^{2+} + 2e^{-} \quad (2)$$

$$2H_2O + 2e^{-} \rightarrow H_2 + 2(OH)^{-} \quad (3)$$

$$Mg^{2+} + 2(OH)^{-} \leftrightarrow Mg(OH)_2 \quad (4)$$

$$Mg^{2+} + 2Cl^{-} = MgCl_2 \quad (5)$$

In nanometer distance to the substrate surface, another reaction takes place:[32]

$$Mg + 2H_2O \rightarrow MgO + H_2\uparrow \quad (6)$$

$Mg(OH)_2$ deposited on the surface has a certain barrier effect, but it is not dense enough to provide effective protection against corrosion. The oxide film may react with Cl^- in the solution, then the film will be penetrated, and Cl^- corrodes Mg to generate $MgCl_2$. Yet, insoluble phosphates and carbonates corrosion products usually deposited as a result of a reaction between Mg and the SBF solution or surrounding tissue fluids, which may act as an auxiliary anti-corrosion layer.[33,34] The above theory can to some extent explain the changes in the *in vivo* and *in vitro* degradation rate of magnesium over time.

3.2. Factors associated with above-mentioned degradation performance changes

Based on the results above, we further focused to find out which aspects of *in vivo* and *in vitro* results are consistent among the changes of magnesium rods degradation behavior caused by increasing grooves. The results of *in vivo–in vitro* correlations are presented in Fig. 4. First, in terms of the corrosion rate, a correlation between *in vitro* and *in vivo* data at 24 weeks was found with a Pearson correlation coefficient (R^2) 0.42 ($p < 0.01$), while there was no linear correlation between the *in vitro* and *in vivo* corrosion rate at 12 weeks. On the other hand, the Pearson correlation-based comparison between the *in vitro* and the *in vivo* degradation volume ratio revealed a highly significant correlation, with an R^2 of 0.74 from 12 weeks' data ($P < 0.001$), 0.89 from 24 weeks ($P < 0.001$), and 0.75 from total ($P < 0.001$). Thus, researchers or manufacturers who want to adjust the

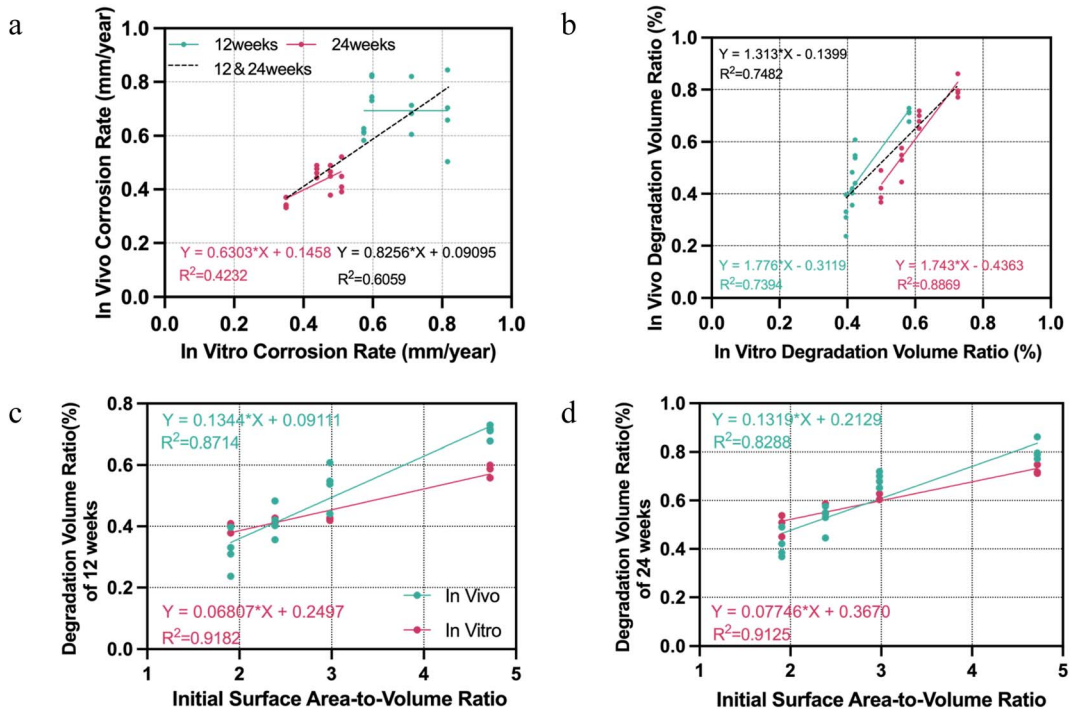

Fig. 4 Analysis of the factors associated with the degradation performance of the HP magnesium rods with different designs. (a) Scatter plot of both *in vitro* and *in vivo* corrosion rate (mm per year) with linear regression prediction lines with statistical significance ($n = 4$). (b) Scatter plot of both *in vitro* and *in vivo* degradation volume ratio with linear regression prediction lines with statistical significance ($n = 4$). (c) Scatter plot of the degradation volume ratio of 12 weeks and initial surface area-to-volume ratio with linear regression prediction lines with statistical significance ($n = 4$). (d) Scatter plot of the degradation volume ratio of 24 weeks and initial surface area-to-volume ratio with linear regression prediction lines with statistical significance.

degradation rate of orthopedic implants through similar structural changes (like adding grooves, threads or holes) were best able to obtain relative degradation volumes, especially over longer periods of time, from *in vitro* immersion experiments, which will help determine the change trend of their degradation rate *in vivo*.

The main structural changes associated with degradation due to differences in the number of grooves is the initial surface area-to-volume ratio. Since the degradation volume ratio is the most consistent parameter reflecting the impact of design changes on the degradation behavior of magnesium rods, regression analysis was performed to analyze the correlation between initial surface area-to-volume ratio and the degradation volume ratio. These results revealed strong positive correlations between initial surface area-to-volume ratio and degradation volume ratio both *in vivo* and *in vitro* at 12 weeks ($R^2 = 0.87$ and 0.92, both $P < 0.001$), which remained consistent at 24 weeks (Fig. 4c and d).

Additionally, the slope of the regression curve for this relationship was significantly greater *in vivo* than *in vitro* in both time points (*t*-test on the regression slope, $p < 0.01$). That is, although we cannot directly calculate the *in vivo* degradation rate from the data of the *in vitro* immersion test, when the surface area-to-volume ratio changes, the relative degradation rate value fluctuates more sharply *in vivo* than *in vitro*, which helps the researchers to determine the possible *in vivo* degradation rate range of the implant after changing the design. For example, if the surface area-to-volume ratio of a HP magnesium implant is reduced by 1 and the remaining volume is reduced by 10% after 12 weeks of immersion tests, then the residual volume reduction after 12 weeks of implantation *in vivo* can be expected to be greater than this amount. It should be pointed out that the linear regression formulas shown in Fig. 4 may not be generalizable to other magnesium-based materials or samples with surface area-to-volume ratio exceeding the range of this experiment.

There have been various studies directed at established an *in vitro* assay to mimic the *in vivo* degradation environment, for example, improving the composition of immersion solution[30] or using dynamic flow,[35] applying static and dynamic loading.[36] This study found that the relationship between *in vivo* degradation performance and *in vitro* degradation rates measured *via* immersion tests varies with the initial surface area-to-volume ratio of the implants. Therefore, experimental groups with samples in different gauge sizes should be added in similar studies aimed at mimicking the degradation behavior of Mg to improve the feasibility of experimental results, rather than only verifying samples of one design and dimension.

3.3. Evaluation of effects of altered surface area-to-volume ratio on peri-implant bone formation

The remaining parts of HP magnesium rods as well as the bone ingrowth within defects at 12/24 weeks of implantation were

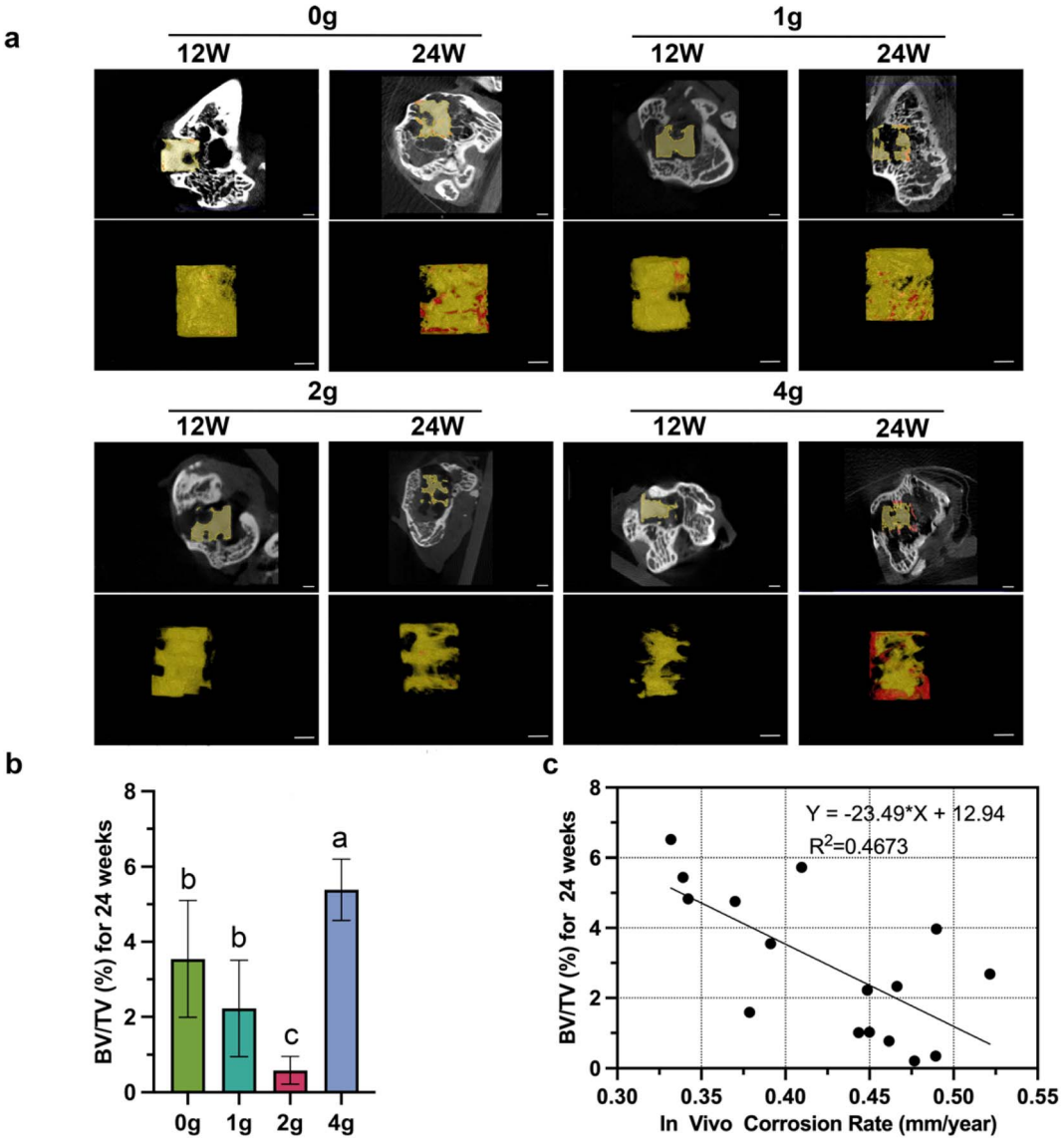

Fig. 5 Micro-CT scanning for *in vivo* imaging of femoral condyle in rats after insertion of HP magnesium rods. (a) 2D and 3D tomography imaging of the implants and surrounding bone tissue at 12 and 24 weeks post-operation. HP magnesium rods: yellow, bone tissue: red. Scale bar: 1 mm. (b) Percentage of bone volume (BV)/total volume (TV) at 24 weeks after operation ($n = 4$). One-way ANOVA with Tukey's *post hoc* test. Columns significantly different letter ($p < 0.05$) to each other would be labeled with different letters. (c) Scatter plot of BV/TV at 24 weeks and *in vivo* corrosion rate (mm per year) with a linear regression prediction line.

shown in Fig. 5a. The pitting type of uneven corrosion were found in all groups of samples. Minimal new bone formation was seen in all groups which is probably due to the excessive accumulation of magnesium ions or release of hydrogen gas, while differences between the groups were still statistically significant (Fig. 5b). Linear regression showing a negative correlation between the *in vivo* corrosion rate and the BV/TV value ($R^2 = 0.47$, $p < 0.01$, Fig. 5c). On the contrary, similar correlations were not observed when applying absolute or relative degradation volume as descriptive data.

To verify the above Micro-CT results, we further analyzed histological staining for the implants retrieved at 12 and 24 weeks postoperatively (Fig. 6). All images were taken from the outer third of the bone tissue surrounding the non-grooved area of the rods. The results from H&E and Masson's trichrome staining showed that all four groups exhibited enlargement of the bone tunnel (indicated by the green circle) due to osteolysis at 12 weeks postoperatively, which correspond to the higher corrosion rate at this stage (Fig. 3a). When the degradation process in the femur condyle reached 24 weeks, it was observed that large quantity collagen fiber and continuous thick bone trabeculae formation began to grow into the filling bone defect area along with the further degradation of "0 g" and "4 g" HP magnesium rods. On the other hand, largest bone defect area and broken trabecular meshwork were found in group "2 g", which correspond to the highest corrosion rate of "2 g" rods. Previously, there are various methods for describing the *in vivo* degradation performance in related studies (degradation

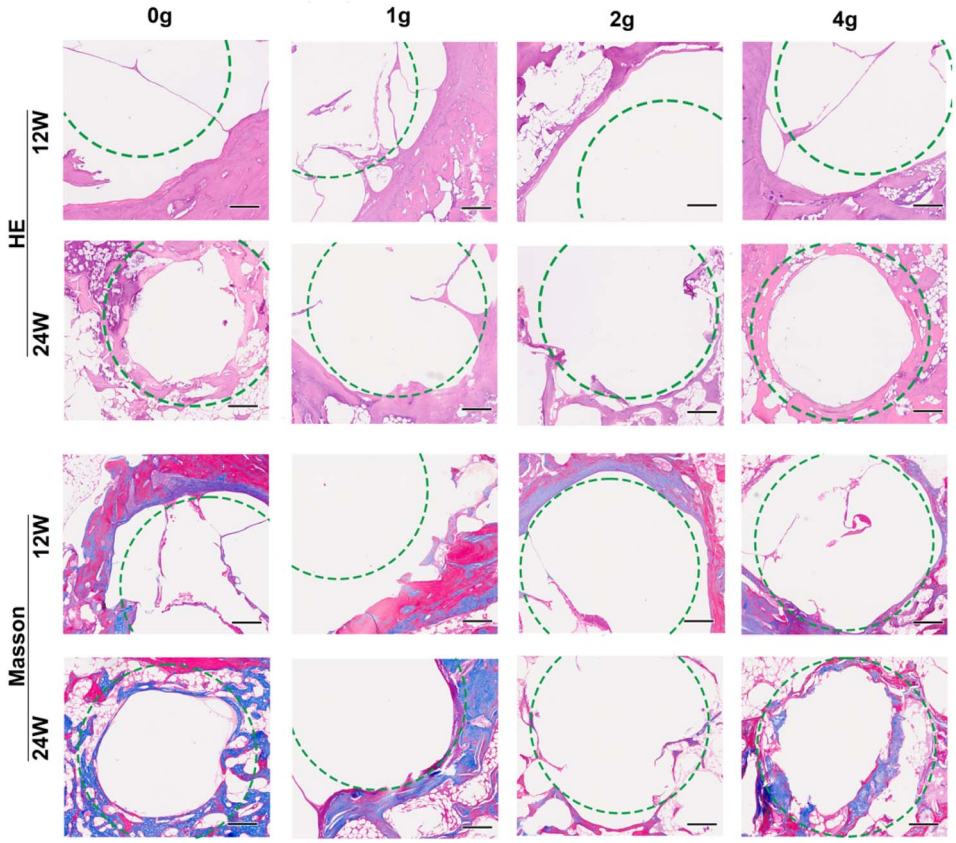

Fig. 6 Representative images of hematoxylin and eosin staining and Masson's trichrome staining. Collagen fiber: blue staining, immature bone tissue: red-blue staining, mature bone: red staining, initial bone tunnel boundary: green circle, Scale bar: 500 μm.

volume, corrosion rate, residual volume percentage and so on). The above results remind us that different description methods are applicable to different evaluation directions.

Findings from this study should be interpreted with limitations in mind. First, only four groups based on differences in surface area volume ratio were set in this study limited by the machining accuracy (φ 3 × 3.5 mm). Second, the absolute values of the size parameters such as the volume and surface area of the HP magnesium rods used in the rats are far from those of most clinical orthopedic implants. Combining the above two points, the results of some tests such us the above regression formula cannot be directly applied to predict *in vivo* degradation performance of clinical implants. Further relevant research (more Mg alloys, larger implants, *etc.*) is still needed to validate the various quantitative relationships involved in this article.

4 Conclusion

The conclusion of this study can be summarized in the following three points.

(1) The increased number of grooves on the HP magnesium surface represented a decrease in the percentage of residual volume over time, not necessarily an increase in absolute degradation volume or a regular change in corrosion rate.

(2) There were strong linear correlations between the relative degradation volume and the initial surface-to-volume ratio of HP magnesium rods both *in vitro* and *in vivo*. The difference in the slope of this relationship *in vitro* and *in vivo* might help to determine the possible range of *in vivo* degradation rates *via in vitro* data.

(3) The corrosion rate is more suitable for evaluating the negative effects of excessive Mg ions and hydrogen release on bone formation compared to the absolute degradation volume.

Ethical statement

All experimental designs and protocols involving animals were approved by the Animal Ethics Committee Peking University Institutional Review Board Office and complied with the recommendations of the academy's animal research guidelines.

Data availability

The datasets used and/or analysed during the current study are available from the corresponding author on reasonable request.

Author contributions

Jiang Sun: investigation, data curation, writing – original draft. Shan-Shan Liu: investigation, data curation. Da Zou: methodology. Xuan He: conceptualization. Jia-You Zhang: data curation. Wei-Shi Li & Zhang-Zhi Shi: writing – review & editing.

Conflicts of interest

There is no known competing financial interests or personal relationships that could have appeared to influence the work reported in this paper.

Acknowledgements

This work was supported by the Key Clinical Projects of Peking University Third Hospital (Grant No. BYSY2022064) and Research and Application of Clinical Diagnosis and Treatment Technology Foundation of Beijing (Grant No. Z201100005520073).

References

1 H. Maradit Kremers, D. R. Larson, C. S. Crowson, W. K. Kremers, R. E. Washington, C. A. Steiner, W. A. Jiranek and D. J. Berry, Prevalence of Total Hip and Knee Replacement in the United States, *J. Bone Jt. Surg., Am. Vol.*, 2015, **97**(17), 1386–1397.

2 Y. Yang, C. He, E. Dianyu, W. Yang, F. Qi, D. Xie, L. Shen, S. Peng and C. Shuai, Mg bone implant: Features, developments and perspectives, *Mater. Des.*, 2020, **185**, 108259.

3 Y. Zhang, J. Xu, Y. C. Ruan, M. K. Yu, M. O'Laughlin, H. Wise, D. Chen, L. Tian, D. Shi, J. Wang, S. Chen, J. Q. Feng, D. H. Chow, X. Xie, L. Zheng, L. Huang, S. Huang, K. Leung, N. Lu, L. Zhao, H. Li, D. Zhao, X. Guo, K. Chan, F. Witte, H. C. Chan, Y. Zheng and L. Qin, Implant-derived magnesium induces local neuronal production of CGRP to improve bone-fracture healing in rats, *Nat. Med.*, 2016, **22**(10), 1160–1169.

4 Y. Wang, Z. Geng, Y. Huang, Z. Jia, Z. Cui, Z. Li, S. Wu, Y. Liang, S. Zhu, X. Yang and W. W. Lu, Unraveling the osteogenesis of magnesium by the activity of osteoblasts in vitro, *J. Mater. Chem. B*, 2018, **6**(41), 6615–6621.

5 D. T. Chou, D. Hong, P. Saha, J. Ferrero, B. Lee, Z. Tan, Z. Dong and P. N. Kumta, In vitro and in vivo corrosion, cytocompatibility and mechanical properties of biodegradable Mg-Y-Ca-Zr alloys as implant materials, *Acta Biomater.*, 2013, **9**(10), 8518–8533.

6 H. Qin, Y. Zhao, Z. An, M. Cheng, Q. Wang, T. Cheng, Q. Wang, J. Wang, Y. Jiang, X. Zhang and G. Yuan, Enhanced antibacterial properties, biocompatibility, and corrosion resistance of degradable Mg-Nd-Zn-Zr alloy, *Biomaterials*, 2015, **53**, 211–220.

7 P. Cheng, P. Han, C. Zhao, S. Zhang, H. Wu, J. Ni, P. Hou, Y. Zhang, J. Liu, H. Xu, S. Liu, X. Zhang, Y. Zheng and Y. Chai, High-purity magnesium interference screws promote fibrocartilaginous entheses regeneration in the anterior cruciate ligament reconstruction rabbit model via accumulation of BMP-2 and VEGF, *Biomaterials*, 2016, **81**, 14–26.

8 U. Thormann, V. Alt, L. Heimann, C. Gasquere, C. Heiss, G. Szalay, J. Franke, R. Schnettler and K. S. Lips, The biocompatibility of degradable magnesium interference screws: an experimental study with sheep, *BioMed Res. Int.*, 2015, **2015**, 943603.

9 D. Chen, Y. He, H. Tao, Y. Zhang, Y. Jiang, X. Zhang and S. Zhang, Biocompatibility of magnesium-zinc alloy in biodegradable orthopedic implants, *Int. J. Mol. Med.*, 2011, **28**(3), 343–348.

10 D. Zhao, S. Huang, F. Lu, B. Wang, L. Yang, L. Qin, K. Yang, Y. Li, W. Li, W. Wang, S. Tian, X. Zhang, W. Gao, Z. Wang, Y. Zhang, X. Xie, J. Wang and J. Li, Vascularized bone grafting fixed by biodegradable magnesium screw for treating osteonecrosis of the femoral head, *Biomaterials*, 2016, **81**, 84–92.

11 Syntellix, *First Magnezix® Surgery in Iran*, 2016, **http://www.syntellix.de/en/newspr/latest-news/single-view/?tx_news_pi1%5Bnews%5D=34&cHash=33ce6146dee249f62675bf26b6d746da**.

12 U&I, *Melting Bone Implant Approved by KFDA*, 2015, **http://www.whowired.com/407024.htm**.

13 CDFA, *Results of Special Approval Application Review for Innovative Medical Devices*, 2014, **https://www.cmde.org.cn/xwdt/shpgzgg/cxyxgsh/20141103151700965.htm**.

14 E. Payr, Beiträge zur Technik der Blutgefäss- und Nervennaht nebst Mittheilungen über die Verwendung eines resorbirbaren Metalles in der Chirurgie, *Arch. Klin. Chir.*, 1900, **38**, 67–93.

15 A. H. Martinez Sanchez, B. J. Luthringer, F. Feyerabend and R. Willumeit, Mg and Mg alloys: how comparable are in vitro and in vivo corrosion rates? A review, *Acta Biomater.*, 2015, **13**, 16–31.

16 E. P. S. Nidadavolu, F. Feyerabend, T. Ebel, R. Willumeit-Romer and M. Dahms, On the Determination of Magnesium Degradation Rates under Physiological Conditions, *Materials*, 2016, **9**(8), 627.

17 N. T. Kirkland, N. Birbilis and M. P. Staiger, Assessing the corrosion of biodegradable magnesium implants: a critical review of current methodologies and their limitations, *Acta Biomater.*, 2012, **8**(3), 925–936.

18 Z. Li, Z.-Z. Shi, Y. Yan, D. Zhang, K. Yang, H.-F. Li, H. Zhang and L.-N. Wang, Suppression mechanism of initial pitting corrosion of pure Zn by Li alloying, *Corros. Sci.*, 2021, **189**, 109564.

19 Z. Yuan, Z. Wan, C. Gao, Y. Wang, J. Huang and Q. Cai, Controlled magnesium ion delivery system for in situ bone tissue engineering, *J. Controlled Release*, 2022, **350**, 360–376.

20 J. Zhang, L. Tang, H. Qi, Q. Zhao, Y. Liu and Y. Zhang, Dual Function of Magnesium in Bone Biomineralization, *Adv. Healthcare Mater.*, 2019, **8**(21), e1901030.

21 W. Qiao, K. H. M. Wong, J. Shen, W. Wang, J. Wu, J. Li, Z. Lin, Z. Chen, J. P. Matinlinna, Y. Zheng, S. Wu, X. Liu, K. P. Lai, Z. Chen, Y. W. Lam, K. M. C. Cheung and K. W. K. Yeung, TRPM7 kinase-mediated immunomodulation in macrophage plays a central role in magnesium ion-induced bone regeneration, *Nat. Commun.*, 2021, **12**(1), 2885.

22 M. F. Ulum, W. Caesarendra, R. Alavi and H. Hermawan, In-Vivo Corrosion Characterization and Assessment of Absorbable Metal Implants, *Coatings*, 2019, **9**(5), 282.

23 W. Liu, X. Li, Y. Jiao, C. Wu, S. Guo, X. Xiao, X. Wei, J. Wu, P. Gao, N. Wang, Y. Lu, Z. Tang, Q. Zhao, J. Zhang, Y. Tang, L. Shi and Z. Guo, Biological Effects of a Three-Dimensionally Printed Ti6Al4V Scaffold Coated with Piezoelectric BaTiO3 Nanoparticles on Bone Formation, *ACS Appl. Mater. Interfaces*, 2020, **12**(46), 51885–51903.

24 C. Rossig, N. Angrisani, P. Helmecke, S. Besdo, J. M. Seitz, B. Welke, N. Fedchenko, H. Kock and J. Reifenrath, In vivo evaluation of a magnesium-based degradable intramedullary nailing system in a sheep model, *Acta Biomater.*, 2015, **25**, 369–383.

25 N. Wojtowicz, I. Danis, F. Monies, *et al.*, The influence of cutting conditions on surface integrity of a wrought magnesium alloy, *Procedia Eng.*, 2013, **63**, 20–28.

26 J. C. Outeiro, A. C. Batista and M. J. Marques, Residual stresses induced by dry and cryogenic cooling during machining of AZ31B magnesium alloy, *Adv. Mater. Res.*, 2014, **996**, 658–663.

27 Z. Pu, J. C. Outeiro, A. C. Batista, *et al.*, Surface integrity in dry and cryogenic machining of AZ31B Mg alloy with varying cutting edge radius tools, *Procedia Eng.*, 2011, **19**, 282–287.

28 S. Desai, N. Malvade, R. Pawade, *et al.*, Effect of high speed dry machining on surface integrity and biodegradability of Mg-Ca1. 0 biodegradable alloy, *Mater. Today: Proc.*, 2017, **4**(6), 6718–6727.

29 M. S. Uddin, H. Rosman, C. Hall, *et al.*, Enhancing the corrosion resistance of biodegradable Mg-based alloy by machining-induced surface integrity: influence of machining parameters on surface roughness and hardness, *Int. J. Adv. Des. Manuf. Technol.*, 2017, **90**, 2095–2108.

30 J. Walker, S. Shadanbaz, N. T. Kirkland, E. Stace, T. Woodfield, M. P. Staiger and G. J. Dias, Magnesium alloys: predicting in vivo corrosion with in vitro immersion testing, *J. Biomed. Mater. Res., Part B*, 2012, **100**(4), 1134–1141.

31 M. Razavi and Y. Huang, Assessment of magnesium-based biomaterials: from bench to clinic, *Biomater. Sci.*, 2019, **7**(6), 2241–2263.

32 A. Kopp, T. Derra, M. Muther, L. Jauer, J. H. Schleifenbaum, M. Voshage, O. Jung, R. Smeets and N. Kroger, Influence of design and postprocessing parameters on the degradation behavior and mechanical properties of additively manufactured magnesium scaffolds, *Acta Biomater.*, 2019, **98**, 23–35.

33 L. Li, M. Zhang, Y. Li, J. Zhao, L. Qin and Y. Lai, Corrosion and biocompatibility improvement of magnesium-based alloys as bone implant materials: a review, *Regener. Biomater.*, 2017, **4**(2), 129–137.

34 H. Wang and Z. Shi, In vitro biodegradation behavior of magnesium and magnesium alloy, *J. Biomed. Mater. Res., Part B*, 2011, **98**(2), 203–209.

35 O. Jung, D. Porchetta, M. L. Schroeder, M. Klein, N. Wegner, F. Walther, F. Feyerabend, M. Barbeck and A. Kopp, In Vivo Simulation of Magnesium Degradability Using a New Fluid Dynamic Bench Testing Approach, *Int. J. Mol. Sci.*, 2019, **20**(19), 4859.

36 Y. Koo, H. B. Lee, Z. Dong, R. Kotoka, J. Sankar, N. Huang and Y. Yun, The Effects of Static and Dynamic Loading on Biodegradable Magnesium Pins In Vitro and In Vivo, *Sci. Rep.*, 2017, **7**(1), 14710.